Comparison of Ternary Bilayer Mixtures with Asymmetric or Symmetric Unsaturated Phosphatidylcholine Lipids by Coarse Grained Molecular Dynamics Simulations

C. Rosetti*,[†,‡] and C. Pastorino[†,‡]

[†]Departamento de Física, Centro Atómico Constituyentes CNEA, Av. Gral. Paz 1499, 1650 San Martín, Buenos Aires, Argentina
[‡]CONICET, Avda. Rivadavia 1917, C1033AAJ Cdad. de Buenos Aires, Buenos Aires, Argentina

ABSTRACT: We studied the phase behavior of various ternary bilayer mixtures composed of cholesterol, an unsaturated lipid, and a fully saturated lipid, by means of molecular dynamics simulations of the MARTINI[1] coarse grain model. We aimed at comparing lateral organization and local properties of bilayers containing phosphatidylcholine (PC) lipids, either with two unsaturated tails (symmetric), or one unsaturated and one saturated tail (asymmetric), as the low-melting component of the mixture. The number of unsaturations per chain was systematically varied in both classes of unsaturated lipids, to account for its consequences in segregation. In the asymmetric unsaturated PCs, the saturated tail was kept identical to the hydrophobic chains of the fully saturated lipid component. Membranes with a symmetric or an asymmetric unsaturated lipid, with the same kind of unsaturated chain, show different phase behavior. Symmetric polyunsaturated PCs set the separation in two phases. Instead, the asymmetric polyunsaturated lipids induced nonideal mixing of components in single-phase bilayers. A significative drop of temperature, within the accessible temperature range, enhances the segregation in mixtures with the more unsaturated asymmetric PC, but still within a single phase. This different phase behavior between membranes with symmetric and asymmetric unsaturated PCs is also observed for lipids with the same total number of unsaturations. On the other hand, the degree of unsaturation per se enhances the segregation, by increasing the composition fluctuations in single-phase membranes with asymmetric PC lipids, and raising the line tension in the two-phase bilayer mixtures with symmetric polyunsaturated PCs. Dynamic clusters of unsaturated asymmetric lipids can be identified. The clusters show no correlation between leaflets, as observed for the phase domains in mixtures with the symmetric polyunsaturated PCs. Interestingly, we found that asymmetric PC lipids have a preferential orientation such that their saturated tails increase their density toward the periphery of the clusters, facing regions enriched in the fully saturated lipids and cholesterol. The degree of unsaturation increases the cluster size and also enhances the anisotropy of the orientation. The surface density of cholesterol follows a gradient that favors its interaction with the saturated tails. Such gradients in composition lead to gradients in order parameters, such as the conformational order and the area of the tails, which increases away from the unsaturated lipid clusters. We compared, in addition, differences in hydrophobic length mismatch between acyl chains of the low-melting and high-melting components, in mixtures containing either symmetric or asymmetric unsaturated lipids.
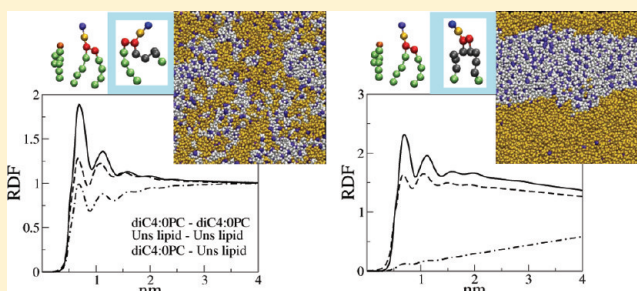
I. INTRODUCTION

Membrane lipids are now recognized not just as a fluid homogeneous support for proteins as was thought once, but rather as active biological elements.[2] A more current picture describes the plasma membrane as an inhomogeneous distribution of lipids and proteins, in dynamic structures spanning length scales from a few to hundreds of nanometers.[3–5] The most common experimental models for natural membranes are lipid vesicles formed with mixtures of cholesterol, a high-melting temperature lipid, and a low-melting temperature, usually unsaturated lipid. These systems can phase separate into two macroscopic liquid phases, named liquid-disordered and liquid-ordered, which differ in their composition and order parameters. The former is enriched in unsaturated lipids, typically with more disordered conformations, while the latter is enriched in well-ordered saturated lipids and cholesterol.[6]

Nevertheless, analogous large-scale separation in natural membranes is seemingly triggered only after the interaction with different chemical signals.[7,8] In resting cells, it has been postulated the existence of stationary nanodomains, whose nature is still under debate.[9] Both out-of-equilibrium processes[10] and equilibrium thermodynamic states[11] have been proposed to explain the short length scale of natural domains. Some authors attribute a fundamental role to membrane proteins in determining the small cluster size.[12]

Interestingly, in lipid-only phase diagrams, the nature of the low-melting lipids has been found to influence domain size. As an example, the phase diagram of ternary mixtures that contain

the diunsaturated lipid dioleoilphosphatidilcholine, DOPC, has two coexisting fluids phases with micrometer-scale separated domains.[6,13] Nonetheless, other mixtures that contain asymmetric monounsaturated phospholipids, with a saturated palmitoyl or stearoyl acyl tail and an unsaturated oleoyl acyl chain (POPC or SOPC), were found to exhibit only small (nano) domains.[14−18] In a very interesting recent publication, Heberle and co-workers have found evidence that these domains can be described as a nanoscale two-phase coexistence.[19] Moreover, a morphologic transition from nanoscopic to microscopic domains has been observed in four-component mixtures with cholesterol after a gradual replacement of POPC by DOPC.[20] There are fewer works describing the behavior of mixtures with asymmetric saturated-polyunsaturated lipids, and, up to now, a complete phase diagram has not been determined. The presence of domains with a radius $\lesssim$20 nm was inferred for mixtures with 1-palmitoyl,2-docosahexanoylphosphatidylcholine (C16:0-C22:6PC), sphingomyelin, and cholesterol, based on the observation of a single spectral component in NMR.[21] However, results from pulsed field gradient NMR measurements in mixtures of egg sphingomyelin, cholesterol, and an asymmetric unsaturated phosphatidilcholine showed different results depending on the degree of unsaturation. They found evidence of macroscopic domains when the unsaturated lipid had four or six double bonds, but not for lipids with one or two unsaturations.[22] From the theoretical ground, several works have postulated that asymmetric (hybrid) lipids could act as line-active molecules, decreasing the line tension and leading to finite size clusters. This was first proposed by Brewster et al. for two-phase systems where these lipids were treated as a minor component.[23,24] In subsequent work, Yamamoto et al. delineated a phenomenological mean field model, based on an extension of the Maier−Saupe model for liquid crystals, which describes the behavior of mixtures with fully saturated, asymmetric lipids, and cholesterol.[25,26] The orientation of the asymmetric lipids at the domain boundaries and the ordering of the saturated tails in contact with the liquid-ordered regions would be the cause for the line-tension decrease. In analogy with the behavior of surfactants, it was proposed that asymmetric lipids would have a double role. On one hand, they would be the molecules of one of the bulk phases, and, at the same time, they would behave as surfactants at the domain interface. They further predicted that the capability to stabilize the small domains will be enhanced with a larger degree of unsaturation.[26] Interestingly, recent molecular dynamics simulations showed that small proportions of monounsaturated, but not polyunsaturated, hybrid lipids could decrease the line tension at the interface of liquid ordered−liquid disordered domains by spontaneously binding to the domain boundaries.[27] This finding is in line with the theoretical predictions in refs 23,24.

Atomistic molecular dynamics (MD) simulations of ternary lipid−cholesterol membranes have been unable, up to now, to show two-phase separations, mainly due to the time and size scales required to equilibrate this diffusion-mediated process. A recent different approach, based on a mixed MD−MC simulation in a semigrand canonical ensemble, has provided evidence of two-phase coexistence with an all atom force field.[28] Atomistic simulations have given insight into the differences in the interactions of cholesterol to saturated and unsaturated lipids,[29,30] the structuring at small length scales,[29,31,32] and the initial stages in the lipids demixing.[33] On the other hand, coarse-grained simulations, at the expense of sacrificing some

molecular degrees of freedom, can reach the longer length and time scales required to properly account for phase separation phenomena in binary and ternary membrane systems. The particle-based MARTINI model[1,34] has succeeded in simulating the phase segregation of saturated lipids, polyunsaturated lipids, and cholesterol, with phase properties that fit well with experimental liquid-ordered liquid-disordered domains.[35] Moreover, a self-consistent mean-field model, built on MD simulations, reproduced the composition and "order" of separated domains in ternary lipid−cholesterol mixtures, in agreement with the experimental phase diagram.[36]

In this work, we describe and characterize the structure of mixtures, which contain an asymmetric (saturated−unsaturated) PC lipid, together with a fully saturated PC lipid and cholesterol, by means of MD simulations of patches with area $A \approx$ 400 nm^2. We used the MARTINI coarse-grained model[1,34] to reach long enough time scales for various mixtures. We varied the number of unsaturations (one, two, or four), while keeping the saturated tail of the same length as the fully saturated component. We examined the differences between those bilayers with membrane mixtures with the symmetric unsaturated lipids. The results show differences in the degree of segregation, which decreases in the presence of the asymmetric unsaturated phospholipids. Moreover, we found that the asymmetric lipid molecules adopt an orientation such that the contacts between their saturated tails and the saturated lipids and cholesterol are increased. A description of simulation methods and the molecular model, altogether with some important quantities measured in these simulations, is given in section II. Section III presents the results of the extensive simulations we performed for various ternary compositions, and section IV provides a discussion and the final conclusions.

II. METHODS

A. Model and Simulation Details. Lipid molecules were described using the MARTINI (version 2.0) coarse grained (CG) model,[1,34] which uses an approximate mapping of 4 heavy atoms of the original lipid in a single interaction site, except for ring structures, which require a more detailed mapping of 2−3 non-hydrogen atoms per bead. The non first-neighbor beads interact through a shifted Lennard-Jones potential (LJ) with a cutoff at R_c = 1.2 nm. Charged beads also interact through a screened Coulomb interaction. The electrostatic potential has a relative dielectric constant of ε_{rel} = 15 for explicit screening and is shifted from 0 nm to its cutoff at R_c = 1.2 nm (the same as the LJ potential). Standard and ring particles are classified into four major classes, which in turn contain several subclasses, according to an hydrophilicity scale and the capability of the beads to form hydrogen bonds.[1,34] The bonded potentials include harmonic terms corresponding to stretching and bending degrees of freedom. The bending rigidity is represented as:

$$V_b(\theta_{ijk}) = K_b(\cos(\theta_{ijk}) - \cos(\Theta_0))^2 \qquad (1)$$

where θ_{ijk} is the bond angle formed by three consecutive beads, i, j, and k, and Θ_0 is the equilibrium bond angle.

For all of the lipids used in this work, the topology of the headgroup consists of two charged beads, modeling a phosphatidylcholine (PC) residue, and two sites of intermediate hydrophilicity represent the glycerol-ester moiety. The tails are constituted by 4 or 5 hydrophobic beads, with 0−4 unsaturated bonds, forming the symmetric molecules, diC4:0PC, diC5:1PC,

diC4:2PC, diC5:4PC, or the asymmetric lipids, (C5:1-C4:0)PC; (C4:2-C4:0)PC; (C5:4-C4:0)PC (Figure 1). From
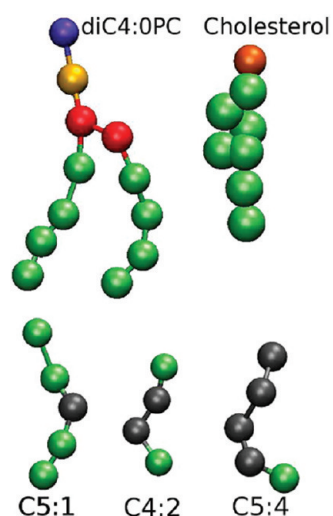
Figure 1. CG representation of the lipids. The phospholipids used in this work, as diC4:0PC, have a phosphatidylcholine headgroup represented by a positively (blue) and a negatively (yellow) charged bead. Two beads of intermediate hydrophilicity (red) are the CG models for the glycerol-ester groups. The acyl hydrocarbon chains have saturated (green) beads and also unsaturated (black) particles, as in the tails showed in the bottom. Cholesterol has a hydrophobic body and a polar bead (orange), which represent the hydroxyl headgroup. The CG acyl chains C4:0, C5:1, C4:2, and C5:4 are approximate models for palmitoyl (C16:0), oleoyl (C18:1), linoleoyl (C18:2), and arachidonoyl (C20:4) acyl chains.

the correspondence of MARTINI beads to heavy atoms, each hydrocarbon bead should represent on average 4 methylenes. The CG C4:0 tail then would represent the all atom (AA) C16:0 palmitoyl chain. The CG C5:1 tail, with an unsaturation in the middle of the chain, roughly corresponds to the oleoyl chain (AA C18:1). The C4:2 chain, with its second and third bead of unsaturated type, is a CG representation of a linoleoyl chain (AA C18:2). Finally, the C5:4 CG tails, with the first four beads unsaturated, represent an arachidonoyl chain (AA C20:4). The unsaturated bonds affect both conformation and flexibility of the lipid chains. These changes are introduced in the model, following the parametrization from refs 1 and 37. The parameters in the bending potential (eq 1) are set to $\Theta_0 = 180°$ and $K_b = 25$ kJ/(mol·rad^2) for the saturated straighter tails, and to $\Theta_0 = 120°$ and $K_b = 45$ kJ/(mol·rad^2) for a kinked tail with a single double bond. To describe the more flexible polyunsaturated chains, the potential parameters of eq 1 are set to $\Theta_0 = 100°$ and $K_b = 10$ kJ/(mol·rad^2).[37] The unsaturated CG beads are more polarizable than the saturated counterparts. In the case of polyunsaturated tails, this leads to unfavorable cross-interaction terms (between saturated C1 type and unsaturated C4 type beads), which are 88% of the self-interaction strength. Nevertheless, the cross- and self-interaction between saturated and unsaturated beads of the monounsaturated lipids (C3 type) are the same. Finally, the parametrization of C5:4 tails has a terminal saturated bead of C2 type, slightly more hydrophilic than the C1 terminal bead of C4:2 tails.

Parametrization of cholesterol was taken from ref 34. The interactions between ring particles are reduced with respect to the interactions between standard particles, by decreasing the effective size ($\sigma = 0.43$ nm instead of $\sigma = 0.47$ nm used for

standard particles), and the effective interaction strength, ε, which is rescaled to 0.75 of that of standard particles. To maintain the rigid structure of the ring, some bonds are connected with high force constants, and another set of bonds is constrained. Moreover, improper dihedral potentials help to keep the molecule in-plane.

All bilayer patches are composed of 1600 lipids, with 562 of each PC lipid type and 476 cholesterol molecules. There are 8.2 water beads per lipid. The composition is initially the same for both leaflets, but fluctuates during the simulations, due to cholesterol flip−flop. We followed the imbalance of cholesterol, quantified as the departure from 1 of the ratio between cholesterol in one and the other leaflet, during the equilibration runs. The average imbalance is around 4% for all of the bilayers, but in some cases there are large fluctuations that can reach a maximum of 14% imbalance. Fluctuations seem similar in magnitude, but faster for the more unsaturated bilayers, although a full characterization would require a deeper study. The equilibration of the bilayers was monitored by the area of the simulation box and the total energy. We also computed the fraction of self-contacts of the saturated PC molecules; this is the ratio of diC4:0PC neighbors over the total number of phospholipid neighbors to a diC4:0PC. This parameter is sensitive to the relative local concentration of lipids, becoming useful to follow the segregation dynamics (see Figure 2). A complete segregation
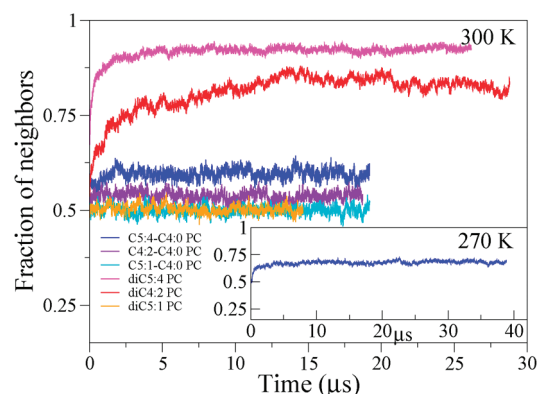
Figure 2. Segregation dynamics in ternary mixtures with diC4:0PC, an unsaturated phospholipid (see legend), and cholesterol. The time evolution is followed with the average fraction of diC4:0PC lipid neighbors over the total phospholipid neighbors of each diC4:0PC lipid. All simulations were run at 300 K, and for the mixture with C5:4-C4:0PC, a simulation at 270 K was also performed (inset).

of the phospholipids will tend to a value of 1. The neighbors of a given lipid were identified by delimiting a Voronoi grid calculated from the phosphate bead of the PC lipids and the hydroxyl bead of cholesterol.

The simulations were run with GROMACS 4.05,[38] in the (N,P,T) ensemble, with a time step of 0.2 ps. A Berendsen thermostat, with a relaxation time of 0.3 ps, was independently applied to the lipids and water to fix the average temperature at 300 or 270 K.[39] The bilayers were simulated in a tensionless state, applying a Parrinello−Rahman barostat with a semi-isotropic scheme, setting the average pressure to 1 bar in the xy plane and z directions. The parameters for the GROMACS implementation of the barostat were set to a coupling time constant of 2 ps and an isothermal compressibility of $\chi = 3 \times 10^{-5}$ bar^{-1}. Following the convention adopted by the authors of the CG model,[1] we report an effective time that is 4-fold the

simulation time, to account for the effective time acceleration due to coarse graining.

B. Analysis. To identify the first-neighbors of a lipid, a Voronoi tessellation was performed, on each leaflet separately, with the voro^{+2}[40] program, configured for two dimensions. The Voronoi grid was computed for the tails, using the position of their center of mass. From the area of the polygonal cells, we estimated the area available for each lipid chain in a particular configuration. Subsequently, we delimited clusters by following the particles connected by at least one common neighbor. To count the clusters of molecules, the Voronoi tessellation was done on the basis of the phosphate bead of PC lipids and the hydroxyl bead of cholesterol.

As a measure of the orientational order of the lipids, we computed an order parameter given by the average second-order Legendre polinomium of the bond angles:

$$P_2(\cos(\theta)) = \left\langle \frac{1}{2}(3\cos^2\theta - 1) \right\rangle$$

where θ is the angle between the bond vector and the normal, $\hat{z}$, to the membrane plane. P_2 ranges from -0.5 to 1, going from a completely perpendicular to a parallel orientation with respect to $\hat{z}$ direction, with 0 corresponding to a random bond distribution. The order parameter of the tails was computed as an average over the bonds formed between consecutive hydrocarbon beads, and between the glycerol-ester beads and the first hydrocarbon beads.

To calculate the 2D surface maps of the density of chains, the order parameter, and the area of the tails (see section III.C), we computed average values on a 40×40 grid, with a bin length of ~0.5 nm. The tails were sorted into the grid cells on the basis of the position of their center of mass. Averages were computed over 24 ns. Within that interval of time, each molecule moves at most its own diameter. Moreover, the rotational autocorrelation function of the vector between the center of mass of the phospholipid tails remains above 20% in all systems. This means that the 2D maps represent a blurred instantaneous configuration of the membranes. Moreover, shorter integration times, of 12 and 4 ns, where at least 40% and 66% of the rotational autocorrelation, respectively, is preserved, show similar characteristics. Meanwhile, differences in the orientation of the lipid tails have almost vanished for time averages longer than 120 ns.

To estimate the degree of correlation between the composition of one and the other membrane leaflet (up–down correlation), we defined the parameter $x = c_u/c_{total}$, as the ratio between the density of unsaturated tails over the density of all phospholipid tails. Density profiles were computed in a grid with bin size ~0.5 nm, and integration time of 24 ns, as described before. We calculated also the covariance coefficient, C_{ua}, between x from the up (x_{up}) and down (x_{dn}) layers of each grid cell:

$$C_{ua} = \langle (x_{up} - \langle x_{up} \rangle)(x_{dn} - \langle x_{dn} \rangle) \rangle / \delta x_{up} \delta x_{dn}$$

where δx_{up} and δx_{dn} are the standard deviations for the x_{up} and x_{dn} values. $C_{ua} = 0$ indicates that there is no linear correlation between the variables; $C_{ua} = +1$ and $C_{ua} = -1$, instead, correspond to a linear (positive or negative) correlation. To determine if C_{ua} values were significantly different from 0, we carried out a t test using the following test statistic:

$$t = \langle C_{ua} \rangle / (\delta c_{ua} / \sqrt{n})$$

in those systems where C_{ua} values were normally distributed, according to a Shapiro–Wilk test (p value > 0.01). δc_{ua} is the

standard deviation of C_{ua} values, calculated one per configuration, and n is the number of configurations. The number of degrees of freedom is $n - 1$.

To estimate the mistmatch (M) between the saturated and the unsaturated lipid, we calculated the difference between the length of their hydrophobic chains (l). The extension of each tail (l) was estimated from the density distributions, as the difference between the position of the last hydrocarbon bead and the glycerol-ester bead, taking the position of the maximum density. In the case of the asymmetric lipids, we computed a mismatch value for each of the tails, as they can be largely different:

$$M_u = l_s - l_u$$

where l_s is the average tail length of the saturated lipid, and l_u is the average tail length of the symmetric unsaturated lipid or, in the case of the asymmetric lipids, is the length of the unsaturated tail. In analogy, M_s represents the mismatch between the average tail length of the saturated lipid and the saturated tail of the asymmetric unsaturated lipids.

The line tension (γ) was measured from the difference between the components of the pressure tensor in the directions perpendicular (P_{xx}) and parallel (P_{yy}) to the domain interface, multiplied by the area over which this pressure acts ($L_y L_z$), and divided by 2, to consider the two interfaces per simulation box:

$$\gamma = \frac{1}{2}(P_{xx} - P_{yy})(L_y L_z)$$

We performed a block-average analysis to estimate the correlation time and check that our simulation time was longer than that value. The error was estimated from the uncorrelated measurements.[41]

III. RESULTS

We tested the equilibration of the samples by following the box area and the total energy. As a parameter indicative of the degree of segregation, we also monitored the diC4:0PC fraction of the phospholipids that are neighbors to a diC4:0PC lipid. As expected, the time intervals needed to converge these quantities are significantly dependent on the length scale of the separation, as observed in Figure 2, which also gives an order of magnitude of the kinetics of the separation. For the more homogeneous mixtures, those containing the asymmetric (unsaturated-saturated) lipids or the diunsaturated diC5:1PC, the equilibrium is already reached within the first microsecond. Instead, for mixtures with diC4:2PC and diC5:4PC, which separate into two macroscopic phases, the parameters become stabilized only after 3.5 and 12 μs, respectively. Average quantities were obtained within the last 15 μs of the simulations. An additional simulation was performed at 270 K for a bilayer containing the asymmetric (C5:4-C4:0)PC. At this temperature, water is supercooled and was monitored to avoid freezing. The diffusion of the lipids decreases on average 4 times with respect to the higher temperature at 300 K. After a slow change up to 10 μs, the bilayer showed no further drift. Despite the slow diffusion, over the longer simulation time the lipids moved on average 14 nm of the 20 nm side box.

A. The Symmetric or Asymmetric Nature of the Unsaturated Lipid Affects the Length Scale of the Segregation. Figure 3 shows characteristic configurations, and the $g(r)$ between the center of mass of the glycerol-ester beads, of ternary mixtures formed by the fully saturated PC diC4:0PC, cholesterol, and an unsaturated phospholipid. Membranes with
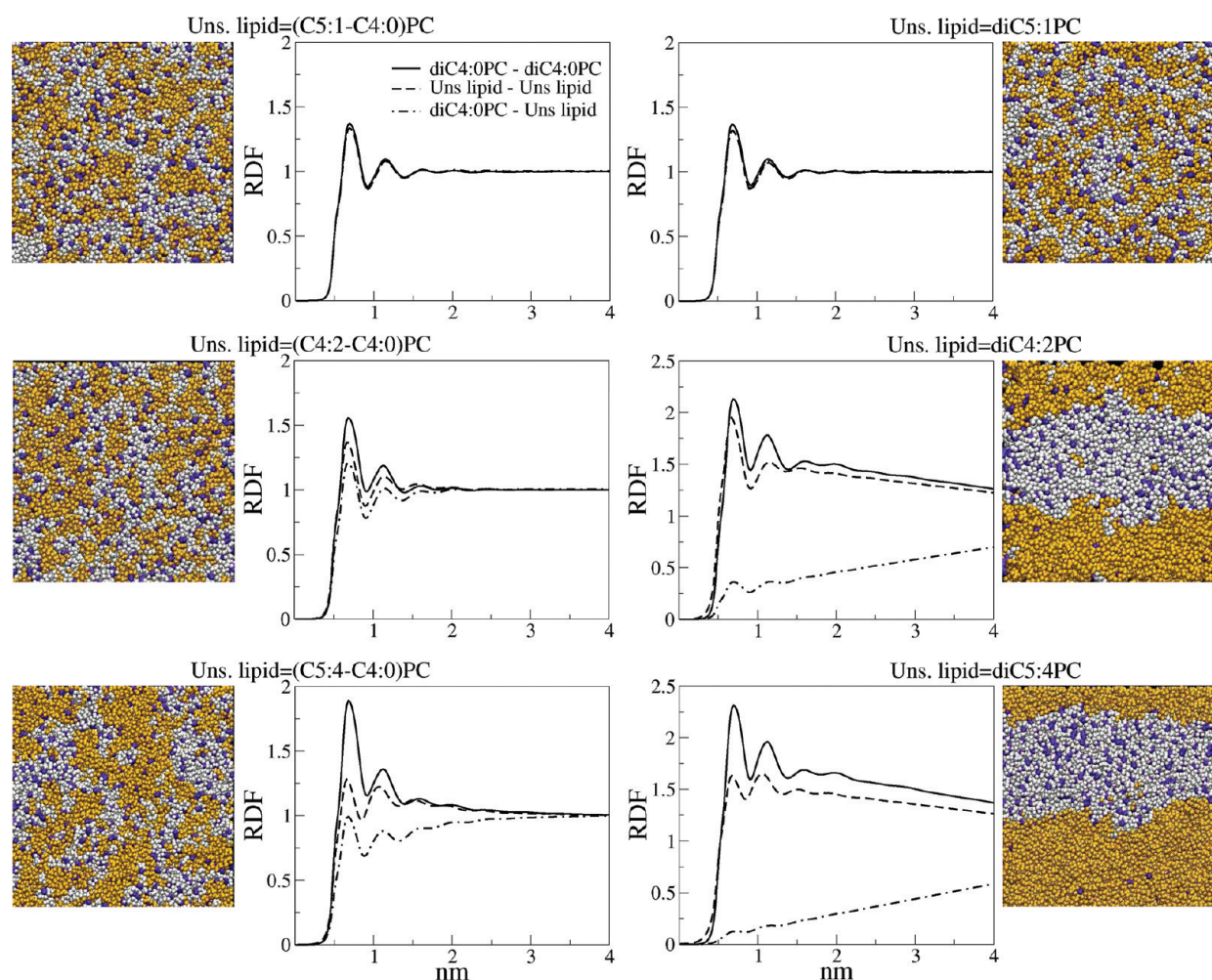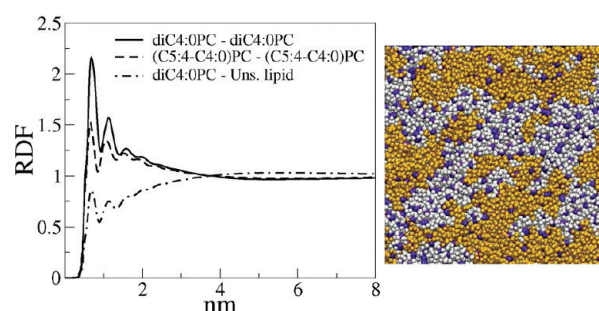
Figure 3. Pair−pair distribution function $g(r)$ between the center of mass of the glycerol-ester beads in 35:35:30 mixtures of diC4:0PC:unsaturated lipid:Chol at 300 K, where the unsaturated lipids are asymmetric (left side graphs) or symmetric (right side graphs) PCs with 1, 2, or 4 double bonds per tail (from top to bottom). The images correspond to representative equilibrium configurations. Color code is light orange for the unsaturated lipid, white for the saturated diC4:0PC, and violet for cholesterol.

unsaturated PC molecules with one, two, or four double bonds in both tails are shown in the right panels of Figure 3, while those containing asymmetric lipids are displayed in the left panels. Changing the composition by replacing the symmetric polyunsaturated PC by the asymmetric polyunsaturated lipids drastically decreases the length scale of the segregation from two-phase mixtures with liquid ordered−liquid disordered domains to single-phase bilayers with nonideal mixing of their components. The radial pair−pair correlation function, $g(r)$ (Figure 3), and also the fraction of contacts depicted in Figure 2 show that the phospholipids are preferably surrounded by lipids of its same type. The $g(r)$ curves, describing the radial distribution of the lipids around themselves, also indicate differences between the packing of diC4:0PC and the polyunsaturated PC components. The $g(r)$ are higher for the fully saturated lipid, and the ratio between the first and the second peak of the radial distributions decreases with the degree of unsaturation. These characteristics are indicative of a better packing of the lipids, and a closer interaction between them, for the more saturated species. In both series of mixtures, with asymmetric or symmetric lipids, the tendency to demix is enhanced by the degree of unsaturation. In the phase-separated bilayers, the line tension increases from 9 ± 3 to 17 ± 3.5 pN for membranes with diC4:2PC to diC5:4PC. This shows up in

the enhanced sharpness of the interface and is consistent with the faster separation dynamics observed in Figure 2. In the membrane mixtures with asymmetric unsaturated lipids, an increased nonideality is observed in the $g(r)$ (Figure 3). A cluster analysis performed on the unsaturated lipid molecules also shows that the cluster size grows with the number of unsaturations (Figure 10 A). In membranes with (C5:4-C4:0)PC, there are large clusters with sizes probably limited by the finite size of the membrane patches, with 281 unsaturated molecules per layer.

The phenomenology of mixtures with cholesterol shows that phase segregation is favored by cooling the mixtures.[6] To account for this, we have also simulated a membrane with (C5:4-C4:0)PC at 270 K instead of 300 K. This temperature is 20 K below the transition temperature of the saturated lipid diC4:0PC.[42] This system does not develop macroscopic domains either, as shown in Figure 3. Nevertheless, the nonideality of the mixture increases with the temperature drop, as observed in $g(r)$ (Figure 4), and in the larger fraction of contacts of the saturated diC4:0PC lipids with themselves (Figure 2). $g(r)$ also shows a slight increase beyond 3.5 nm indicative of a more organized spatial structure within the few nanometers range. It is interesting to compare from this set of results the behavior of lipids with four double bonds. The symmetric

Figure 4. Pair–pair distribution function $g(r)$ between the center of mass of the glycerol-ester beads in 35:35:30 mixtures of diC4:0PC: (C5:4-C4:0)PC:Chol at 270 K. The image is a representative configuration of the bilayer. Color code is the same as that in Figure 3: light orange for the unsaturated lipid, white for the saturated diC4:0PC, and violet for cholesterol.

diC4:2PC shows two-phase separation with a considerable line tension at the interface. Meanwhile, the asymmetric lipid (C5: 4-C4:0)PC induces a nonideal mixing of components in an otherwise single phase membrane, even after decreasing the temperature well below the transition temperature of the saturated component. In an undergoing set of simulations, we observed that mixtures with asymmetric lipids can separate into macroscopic phases by enhancing the mismatch between the lipids. These results will be the subject of a future work.

For the symmetric lipid with monounsaturated tails, the mixture is rather homogeneous (Figure 3), although experimental ternary membranes with dioleoilphosphatidylcholine as the low-melting component show two-phase separation with mole fractions from 15% to 35% of cholesterol.[43] The present parametrization of MARTINI makes the interaction between diC4:0PC and diC5:1PC tails, and between those with cholesterol, rely only on differences in the bending potential, as the LJ parameters are the same. In a recent paper, Domanski and co-workers described nonideal mixing without macroscopic domains (even for lower temperatures) using a slightly different parametrization of the unsaturated beads.[44] This suggests that the mixing between phospholipids will also be overestimated for the asymmetric monounsaturated PC. Despite these probable inaccuracies of the model, we include all of the results seeking for a comprehensive study of the properties of these mixtures as a function of the number of double bonds

B. Unsaturated Asymmetric Lipids Present a Preferred Orientation in Short-Range Transient Domains. The results of this section describe the lateral structure of the different acyl chains in asymmetric PC-containing membranes.

It is interesting to consider first the orientation of cholesterol in these bilayers. In all of the studied bilayer membranes, with a saturated PC and an unsaturated asymmetric PC, we found that the preferred orientation of cholesterol is perpendicular to the interface. This is an expected result, as it is also the preferred orientation in pure membranes of asymmetric highly polyunsaturated lipids, without the saturated PC.[37,45,46] There is however a clear increase, as a function of the degree of unsaturation, of the fraction of cholesterol that resides inside the membrane, lying parallel to the interface. The mole percent of cholesterol molecules with tilts between $60° \leq \theta \geq 120°$ is 0.60 ± 0.02, 1.19 ± 0.03, and 2.50 ± 0.04, for mixtures with unsaturated PCs with one, two, or four double bonds, respectively. The tilt was computed as the angle between the membrane normal and the vector joining the hydroxyl group and the first

carbon-bead linked to the sterol body. The perpendicular orientation is further enhanced in the liquid-ordered separated domains, observed in two-phase mixtures with symmetric polyunsaturated lipids (diC4:2PC and diC5:4PC). Cholesterol molecules with larger tilts are reduced to 0.1% in those tightly packed domains. In contrast, in the liquid-disordered domains of those same membranes, the population of cholesterol lying inside the bilayer increases, as was first described in several previous works.[35,37,45,46] The cholesterol molecules with tilts in the range $60° \leq \theta \geq 120°$ are 39.5 ± 0.5 and 11.5 ± 0.4 for liquid-disordered domains enriched in diC5:4PC and diC4:2PC, respectively. Finally, mixtures with diC5:1PC present cholesterol mostly aligned to the membrane normal.

Regarding the surface arrangement of the lipid tails in bilayers with asymmetric polyunsaturated PCs, a closer look shows a local spatial organization of the different hydrophobic chains (Figures 5 and 6). Unsaturated lipids have a preferential
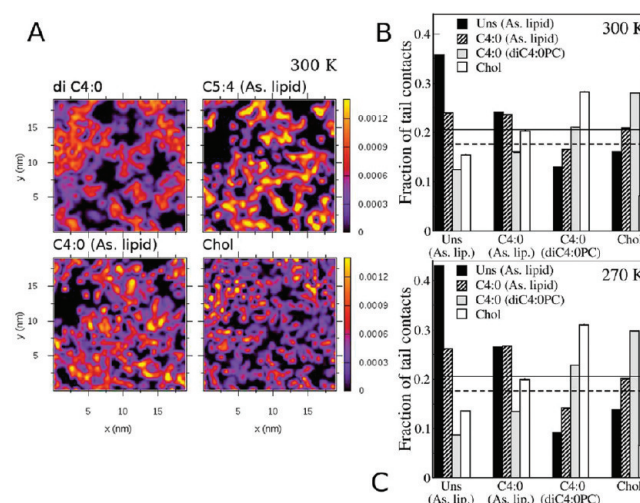
Figure 5. Surface tail densities in 35:35:30 (C5:4-C4:0)-PC:diC4:0PC:Chol ternary mixtures. Values were averaged over 24 ns on a 40 × 40 grid (~0.5 nm bin length). The mean between both tails is presented for diC4:0PC (A). Distribution of tail–tail contacts for each of the tail types indicated in the x axis, at 300 K (B) or 270 K (C). diC4:0PC is represented by the mean between both of its tails. Horizontal black lines are the expected fraction of contacts with any of the PC tails (—) or with cholesterol (– – –), for a completely random distribution.

orientation, which results in a qualitatively different density map for each of their hydrocarbon chains, a tendency that is enhanced with the number of double bonds. Figure 5 shows the 2D density maps for the hydrocarbon chains in membranes with C5:4-C4:0PC, the most unsaturated of the asymmetric lipids studied. Comparing the tails of the asymmetric lipid, C5:4 is observed to clearly have a complementary distribution to diC4:0PC (represented by the average between both of its tails). Instead, C4:0 chains show a broader distribution with a larger overlap with the fully saturated lipid. Such qualitative differences in the distribution are not observed between the identical chains of diC4:0PC (not shown). On the other hand, cholesterol follows a density gradient with enhanced concentration in regions enriched with saturated chains. The resulting spatial organization is better appreciated in Figure 11A, where just one-quarter of the membrane patches are shown: the unsaturated asymmetric lipids have a preferential orientation with their saturated tails facing the diC4:0PC clusters.
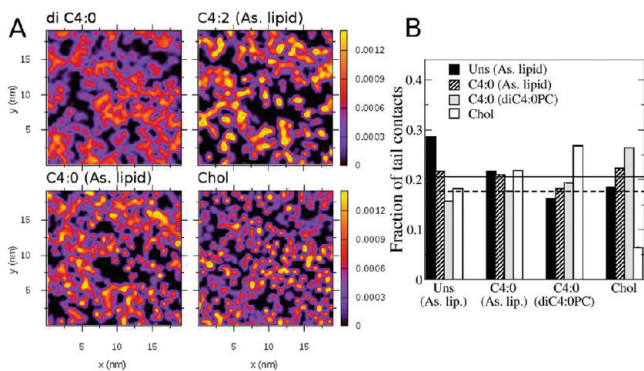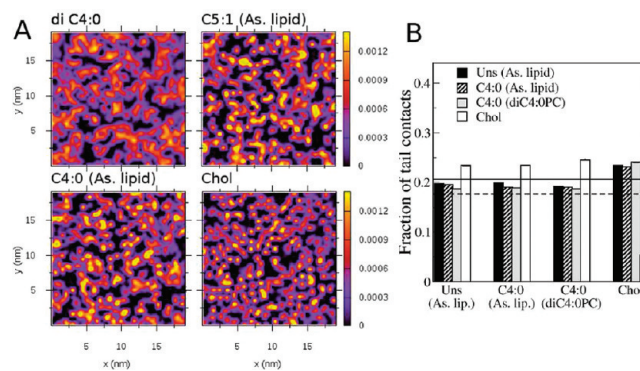
Figure 6. Surface tail density (A) and distribution of contacts between tails (B) for 35:35:30 (C4:2-C4:0):(diC4:0):(Chol) membranes. Details are the same as in Figure 5.

Figure 7. Surface tail density (A) and distribution of contacts between tails (B) for 35:35:30 (C5:1-C4:0):(diC4:0):Chol membranes. Details are the same as in Figure 5.

The average tail−tail contacts between the different tail types in Figure 5 help to further characterize the arrangement of the lipids. We only computed pairs of independent tails, those belonging to different molecules, to obtain a more meaningful deviation from a random distribution. As all four PC tails have the same average proportion, the fraction of contacts with any of them should be the same in the absence of any tail−tail preference. Moreover, in a completely randomized mixture, the contact ratio with any PC tail should be 20.6% (solid horizontal line) and 17.6% with cholesterol (dashed horizontal line). A feature that stands from Figure 5 is the difference in the contact distribution between the unsaturated lipid tails. C5:4 chains have a self-preference that is not observed for C4:0 tails, which have almost the same fraction of contacts with one or the other chain of the unsaturated lipid. Furthermore, although both tails show reduced contacts with diC4:0PC, the trend is more pronounced for the unsaturated chain. The contact-distribution of cholesterol shows a self-avoidance, with a small fraction of contacts with a cholesterol neighbor, in agreement with previous molecular dynamics simulations.[32,35] The results also indicate the preference of cholesterol for the saturated over the unsaturated tails of the asymmetric lipid, as was also found in earlier simulations[47] and NMR experiments.[48,49] Moreover, the most probable cholesterol-contacts are with the saturated chains of diC4:0PC, as is also clear from the observation of the density distribution map (Figure 5). Decreasing the temperature to 270 K enhances these trends (Figure 5C). A greater decrease of unsaturated to saturated lipid contacts is observed. The neighbor population of C5:4 tails becomes even more enriched in unsaturated tails, and deprived of diC4:0PC tails. For cholesterol instead, the opposite takes place: diC4:0PC neighboring tails increase and C5:4 chains concomitantly decrease.

The membrane with C4:2-C40PC (Figures 6 and 12) as the unsaturated lipid shows similar tendencies, although the effects are decreased in magnitude. In bilayers with the monounsaturated C5:1-C4:0PC (Figures 7 and 13), all PC chains show a similar distribution of tail contacts, as a consequence of the good mixing that these systems show in the coarse grain model. Nevertheless, the reduced cholesterol−cholesterol contacts are also observed in this bilayer, although in this case there is no significant preference of cholesterol for diC4:0PC chains over C5:1-C4:0PC tails (Figure 7).

The spatial structure of the mixtures was also analyzed with 2D radial distribution functions, $g(r)$, between all tail−tail center of mass (COM) pairs. Again, only the tails belonging to

different lipid molecules are computed into the $g(r)$ to avoid the intramolecular contributions. Figure 8 compares the results
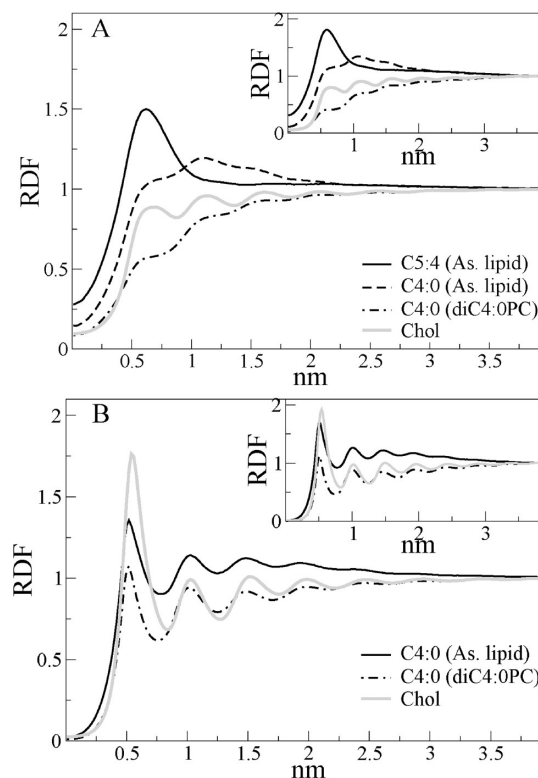
Figure 8. Pair−pair distribution function $g(r)$ between the COM of C5:4 tails (A), or C4:0 tails (B) of (C5:4-C4:0)PC unsaturated lipid, and the COM of the other lipid chains present at 300 K in ternary mixtures with 35:35:30 (C5:4-C4:0):(diC4:0):Chol. The inset shows the curves for the same mixture at 270 K.

for the saturated and the unsaturated tail of (C5:4-C4:0)PC. The first neighbor of an unsaturated tail is preferentially another unsaturated tail whose COM is placed ∼0.6 nm away. This distance is larger than the position of the first C4:0-C4:0 peak, which is ∼0.5 nm, due to the bulkier shape of the unsaturated chains (Figure 8B). The most probable second neighbor is the saturated, C4:0, tail of the asymmetric lipid at ∼1.1 nm (Figure 8A). Notice that these saturated chains are more frequently found in this position than closer to C5:4 tails (the second peak is larger than the first one). This slightly preferred

distance may be due to the fact that an unsaturated tail is usually intercalated in between. Finally, both diC4:0PC tails, and to lesser extent cholesterol, are depleted from the region contiguous to C5:4 hydrocarbon chains. On the contrary, next to the saturated C4:0 tail appears a well-defined and high cholesterol peak. This structure, as shown by the $g(r)$ curves, develops just at short length scales (below 3.5 nm) and is enhanced at lower temperatures (Figure 8, inset). One rather unusual feature of the $g(r)$ curves in Figure 8 is the considerable deviation from zero at $r = 0$. This is particularly noticeable in the $g(r)$ between the COM of highly polyunsaturated chains and is apparently related to the large flexibility of these hydrocarbon tails. From the visual inspection of this membrane, we identified several cases where pairs of tail-centers of mass were aligned in the z direction (contributing to the $g(r)$ at $r = 0$). These corresponded to arrangements where the curved tails of different molecules were entangled with each other, and other cases where the tails, extended somewhat parallel to the interface, were overlapped. These configurations become more accessible for the more polyunsaturated chains, which have a broader range of accessible conformers.[50-53] The average tail order parameter, progresively closer to 0 for the more unsaturated chains (Figure 14), is the result of that increased flexibility. In this same line, we also observed that the deviation from zero in the $g(r)$ at $r = 0$ becomes larger as the distribution of the center of mass of the tails along the z axis becomes wider, which is what happens as the hydrophobic chains become more unsaturated. The $g(r)$ curves of cholesterol for the same mixture are depicted in Figure 9. The cholesterol—cholesterol $g(r)$
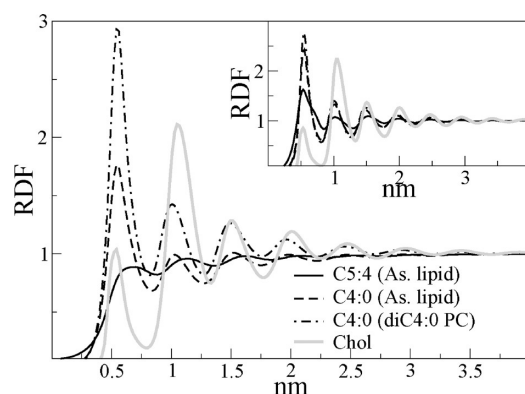

Figure 9. Pair—pair distribution function $g(r)$ between the COM of cholesterol and the COM of the other lipid chains present in ternary mixtures with 35:35:30 (C5:4-C4:0):(diC4:0):Chol, or in membranes with 35:35:30 (C5:1-C4:0):(diC4:0):Chol (inset).

curve is similar to that reported in ref 32, with a first peak much smaller than the second one, indicative of its self-aversion. The large ordering effect induced by cholesterol on the saturated tails is preserved up to three to four molecules away, being more pronounced on the saturated lipid diC4:0PC. Meanwhile, its effect on the unsaturated tails is almost negligible. Regarding the other membranes studied, we found similar trends for the $g(r)$ curves of mixtures with (C4:2-C4:0)PC as the unsaturated lipid (not shown). On the other hand, the monounsaturated PC (C5:1-C4:0)PC shows almost the same $g(r)$ curves between the different pairs of phospholipid tails as a result of the good mixing in the coarse grain model (not shown). Nevertheless, also in these membranes, the order induced by cholesterol is larger on the saturated than over the unsaturated

tails (Figure 9, inset). Furthermore, the cholesterol—cholesterol $g(r)$ distribution is independent of the bilayer composition (compare Figure 9 and inset).

The spatial organization described up to now also influences the size distribution of the tail-clusters. The major effect of increasing the degree of unsaturation is the larger cluster sizes developed, for the unsaturated hydrocarbon chains (Figure 10B).
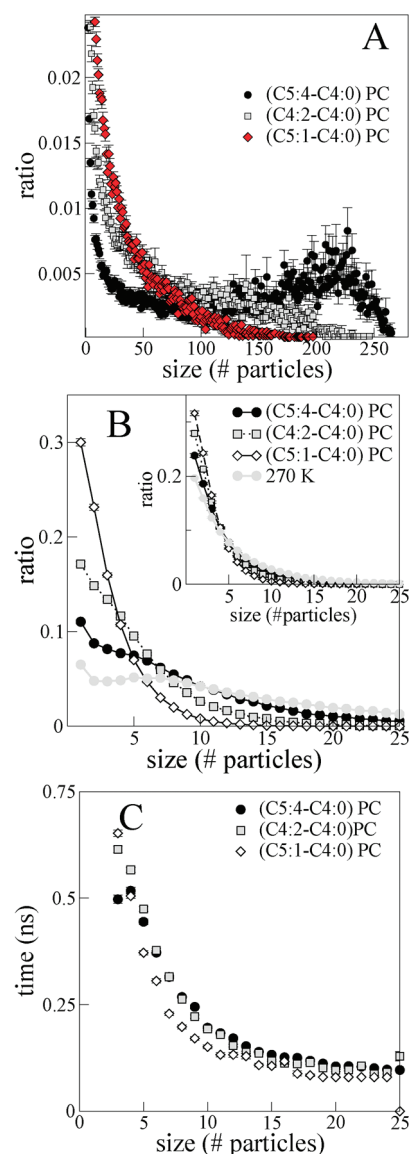
Figure 10. Distribution of clusters of unsaturated lipids (A) or unsaturated tails (B) in ternary mixtures of 35:35:30 diC4:0PC/unsaturated lipid/cholesterol. The ratio is computed on the basis of the number of particles in clusters of a certain size. The inset in panel B shows the distribution of clusters of the saturated tails of the asymmetric lipids. Part C shows the average lifetime of clusters of unsaturated tails as a function of their size.

More subtle differences with the same tendency are followed by the saturated C4:0 tails of the asymmetric lipids (Figure 10B, inset). The effect on the cluster size distribution of each diC4:0PC tail, and of cholesterol, is in turn only slight (not shown).

Next, we analyze if any difference shows up in the cluster dynamics. We followed the tail-clusters, selecting, in each

configuration, the largest number of particles that remained together. These clusters are fluctuating structures that change by the addition or loss of single molecules, and also by the splitting or merging of bigger clusters. The vast majority of them disappear after tens of nanosecond, but some last hundreds of nanosecond. On the other hand, we also determined the average time a cluster remained of a certain size, computing the time-lapse until the cluster size increased or decreased. We calculated these averages over sets of independent clusters. Figure 10C shows these average lifetimes. The curves are decreasing functions, and they are similar for the different membranes, meaning that these times are mainly determined by the cluster size, and not the composition. The baseline in Figure 10C is limited by the mininum time step between analyzed configurations and has no physical meaning.

Finally, we compared the colocalization of the composition in one and the other bilayer leaflet, in mixtures with symmetric or asymmetric PCs with the same unsaturated chain. We tried to observe if the smaller clusters followed the tendency of the larger domains. In Table 1 we show the covariance coefficient,

Table 1. Covariance Coefficient (C_{ua}) between the Composition from the Up and Down Hemilayers, and Mismatch (M) between the Tails of the Saturated and the Unsaturated Lipid^a

	(X-C4:0):diC4:0PC:Chol			(diX):diC4:0 PC:Chol	
	C_{ua}	M_u (nm)	M_s (nm)	C_{ua}	M_u (nm)
X = C5:4 (300 K)	−0.09	0.57(5)	0.04(5)	0.66	0.41(5)
X = C5:4 (270 K)	−0.07	0.64(6)	0.09(6)		
X = C4:2	−0.08	0.31(5)	−0.02(5)	0.60	0.31(5)
X = C5:1	0.005	−0.05(4)	0.02(4)	0.007	0.04(4)

$^a M_s$ represents the mismatch with the saturated tail of the asymmetric lipid, and M_u represents the mismatch with the unsaturated tail of the asymmetric lipid or with both tails of the symmetric unsaturated PC.

C_{ua}, between the composition in the opposing hemilayers. The phase domains are in-register in the macrophase separated membranes. In a previous work, we had also described the up–down correlation in a nonideal binary membrane with diC4:0PC and diC4:2PC due to coupled composition fluctuations.[53] In mixtures with the asymmetric polyunsaturated lipids instead, there is no correlation between hemilayers. The slightly negative deviations are not significant within a probability threshold of 1%. At the lower temperature, C_{ua} is also close to 0. However, in this case, C_{ua} values are not normally distributed, maybe due the slower dynamics and larger fluctuations we observe. A non-departure from 0 cannot be confidently affirmed, but the C_{ua} values range from a minimum to a maximum of −0.2 to 0.12. Last, mixtures with the symmetric or asymmetric lipids having monounsaturated tails, which are rather homogeneously mixed, show no correlation of the composition between leaflets.

Hydrophobic mismatch can influence the interaction in-plane and from one to the other hemilayer. Asymmetric lipids with hydrophobic chains of different nature can have quite different tail lengths. We estimated the mismatch between each tail of the asymmetric lipids and the saturated lipid tails, and compared it to the mismatch between saturated and unsaturated lipid tails in membranes with symmetric PCs (Table 1). No mismatch is measured, within the error, for the saturated tail, but the unsaturated chain presents a mismatch of the same

order as that of the symmetric lipids. Major differences then are found between both tails of the asymmetric PC that greatly increase with the degree of unsaturation.

C. The Order Parameters Vary with the Local Composition of Tails. Figures 11–13 show the surface distribution of tail densities, together with the average orientational order parameter $P_2(\cos(\theta))$ and tail area. We quantified the average values from all phospholipid tails and from the saturated C4:0 tails belonging to diC4:0PC and to the asymmetric unsaturated lipid. The results show that the gradients of composition are followed by rather steep gradients in the conformational order. Figure 11 shows the results for membranes with (C5:4-C4:0)PC. Highly "disordered" regions enriched in the unsaturated C5:4 tails are characterized by low order parameter values, and a loose packing (large tail areas). Moreover, the fluctuations in both quantities, which are independent indicators of conformational disorder, are also large. These are useful complementery data, as a low order parameter value alone may represent a biased sampling toward conformations perpendicular to the interface. Outside these regions, there is a rather steep increase of the order toward areas with high local ratios of saturated tails and cholesterol (Figure 11). Looking solely to the C4:0 tails, we see that the saturated chains alone follow the gradient of order just described.

We have also compared the order parameter distribution between the C4:0 tails of the asymmetric PC and the saturated PC in Figure 14. The asymmetric lipid has shifted values to lower order parameters with respect to those in diC4:0PC. Now, the conformational order of the saturated lipid is not as high as in the two-phase membrane with liquid-ordered phase-separated domains, as is also depicted in Figure 14A. The dispersed clusters of the unsaturated lipid disrupt the order of the liquid-ordered phase. In line with this observation, the diffusion of the saturated lipid is also higher in membranes with the asymmetric unsaturated lipid, with $D = 0.6 \times 10^{-7}$ cm^2 s^{-1} as compared to $D = 0.1 \times 10^{-7}$ cm^2 s^{-1} in the liquid ordered domains.

The bilayer with the less unsaturated lipid C4:2-C4:0PC shows similar characteristics: higher "order" and packing in regions enriched in saturated tails (see Figure 12). A progression in the conformational order is clear from Figure 14B where, as before, the saturated tails reach the more ordered state in the two-phase membrane. In turn, the C4:0 tail of the asymmetric lipids is more disordered on average than diC4:0PC tails in single phase bilayers with (C4:2-C4:0)PC (Figure 14B).

The distribution of $P_2(\cos(\theta))$, represented in Figure 14C, indicates that the orientational order is very similar for the saturated tails that belong either to the asymmetric or to the fully saturated lipid, in ternary membranes with the monounsaturated PC. The distribution is also similar to that in bilayers with the symmetric diC5:1PC. The single double bond decreases the order with respect to the saturated chains, although to a lesser extent than the polyunsaturated tails (compare Figure 14C to A and B). Nevertheless, in the coarse grain model, the effect is not strong enough to induce a differential orientation or distribution for the different saturated tails along the membranes.

IV. DISCUSSION

Asymmetric unsaturated lipids are more widely distributed in natural membranes, whereas lipid species in which both acyl chains are unsaturated are present in much lower proportions in the majority of tissues, with particularly high ratios in specific cell types.[54] Finding differences in their phase behavior is then a
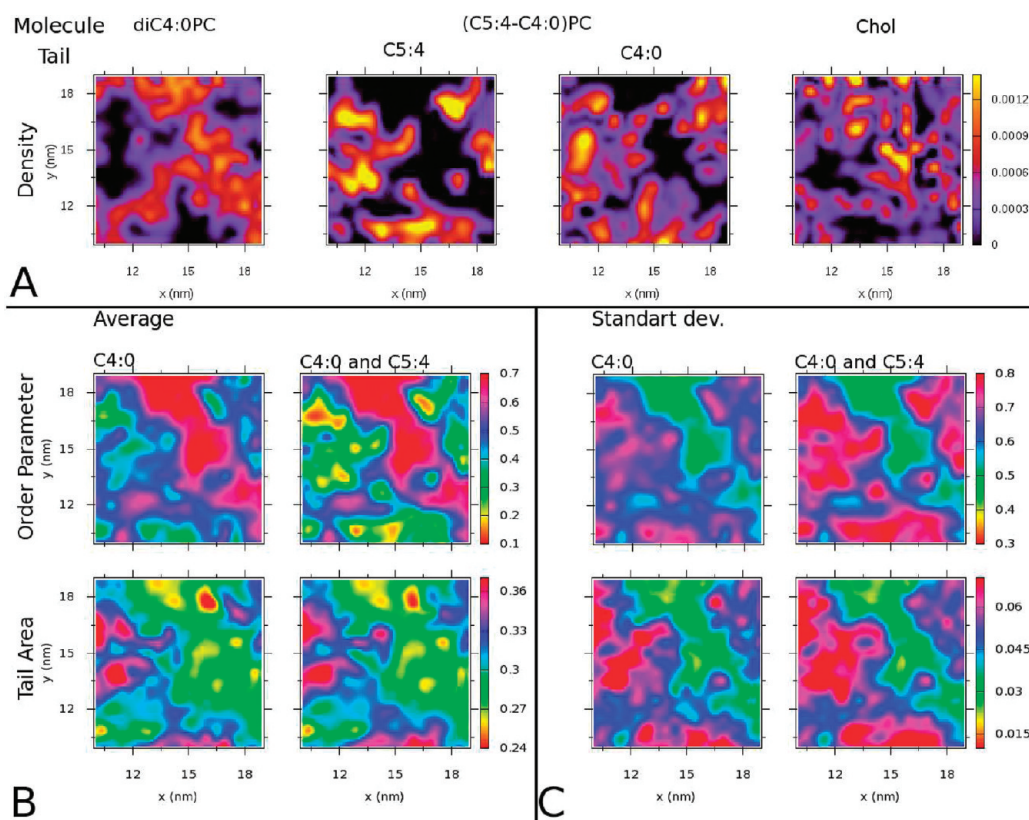
Figure 11. Surface plots of the density, order parameter, and area of the tails, for 35:35:30 (C5:4-C4:0)PC:diC4:0PC:Chol mixtures. Panel A shows the average density of both tails of diC4:0PC, the C5:4 and C4:0 tails of the asymmetric lipid, and cholesterol. Panel B represents the average values, and panel C the standard deviation, for the conformational order parameter ($P_2(\cos\theta)$) and tail area, calculated for the saturated C4:0 tails, including those of the asymmetric unsaturated lipid and diC4:0PC, or for the average over all phospholipid tails (C4:0 plus C5:4). All of the values were calculated over 24 ns on a 40 × 40 grid with ~0.5 nm of bin length. The area was estimated from a Voronoi tesselletion computed from the tails COM.

relevant issue to understand the active role of these lipids in the membrane function.

In the framework of the MARTINI coarse grained model, we compared ternary membranes with cholesterol, which differ solely in the low-melting unsaturated component, taking as a mean difference the presence of unsaturations in one (asymmetric lipid) or both (symmetric lipid) of the unsaturated lipid hydrocarbon chains. We focused on the differences in lateral organization and scale, the order parameters, and some dynamic characteristics of these mixtures. In both classes of lipids, we changed the number of unsaturated beads per chain, and, for the asymmetric PC, we kept the same saturated tail as the hydrophobic chain of the fully saturated lipid.

Our simulations show that increasing the degree of unsaturation enhances the tendency to demix, in agreement with experimental results,[21] and this trend shows up for both classes of unsaturated lipids. Bilayers with cholesterol and polyunsaturated symmetric lipids show two-phase domains.[35] Instead, mixtures with asymmetric lipids with the same unsaturated chain show one single phase, which becomes increasingly nonideal with the number of unsaturations. This different phase behavior also holds when comparing lipids with the same number of unsaturations per molecule. Decreasing temperature well below the melting temperature of the saturated lipid, which is a known trigger factor for liquid–liquid immiscibility,[6] reinforces further this observation: although demixing is enhanced, no macroscopic separation was observed under this condition. This observations are in agreement with experimental results by

Konyakhina et al., showing that increasing the fraction of the symmetric unsaturated lipid DOPC, with respect to the asymmetric POPC, in mixtures with cholesterol drives the pattern from nanoscopic to microscopic domains.[20] Moreover, the small clusters lose any correlation between both hemilayers, as it is actually found for membrane domains in mixtures with a symmetric polyunsaturated PC.[35,53,55]

We identify at least two factors that could contribute to this mixing behavior, both possibly having their origin in that the different classes of tails in the asymmetric lipid show different properties and behavior. One of them is the mismatch between the saturated and polyunsaturated lipids, which will promote the segregation.[44] In bilayer mixtures with asymmetric lipids, the hydrophobic lengths of all of the saturated tails, those in the saturated and the unsaturated lipid, are all similar. A large mismatch is only established with the polyunsaturated tail. The second is that asymmetric lipids can adopt a short-range arrangement, which may help with the mixing of the lipids (see below).

The change from macroscopic to nanoscopic domains is observed in experiments, upon replacing a symmetric PC by an asymmetric PC.[14−16,18] The exact nature of the nanoscale domains has not been elucidated yet, and their stabilization possibly requires an effective long-range force.[56] Still, this phenomenon requires enhanced mixing between the lipids. In this line, some of our results suggest that the asymmetry of the low melting lipid may per se favor a decrease of the segregation length scale, as was proposed in refs 23−26.
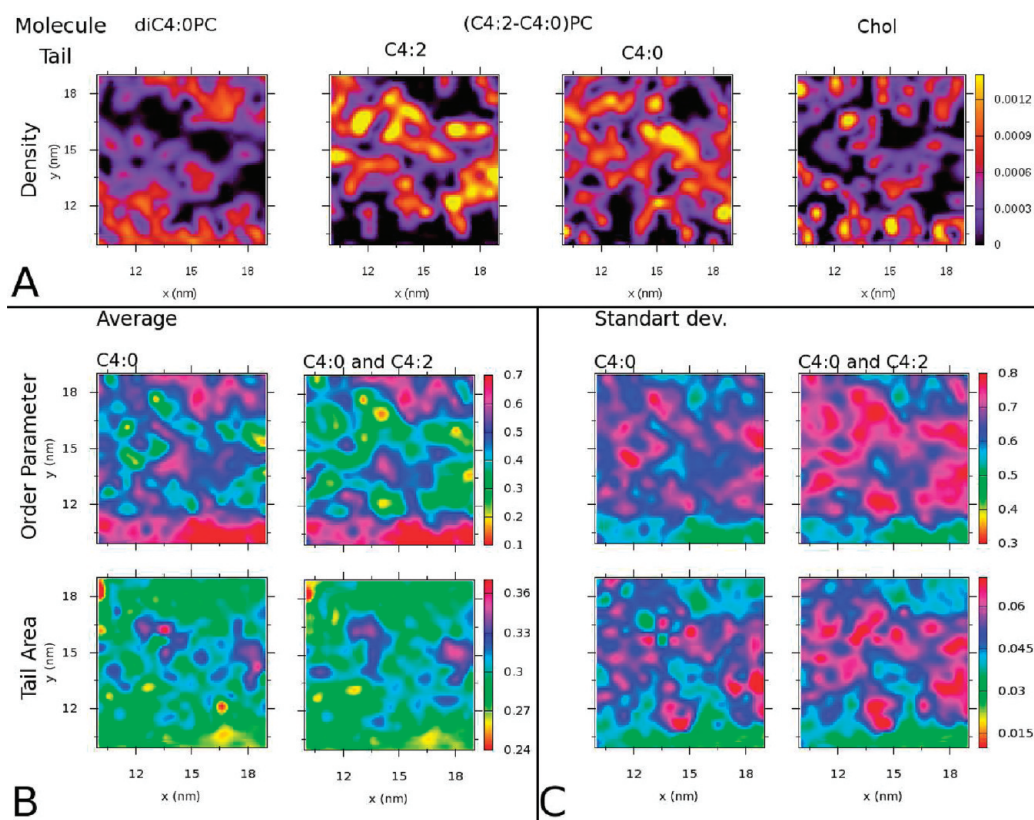
Figure 12. Surface plots for 35:35:30 (C4:2-C4:0)PC:diC4:0PC:Chol mixtures. Details are the same as in Figure 11.
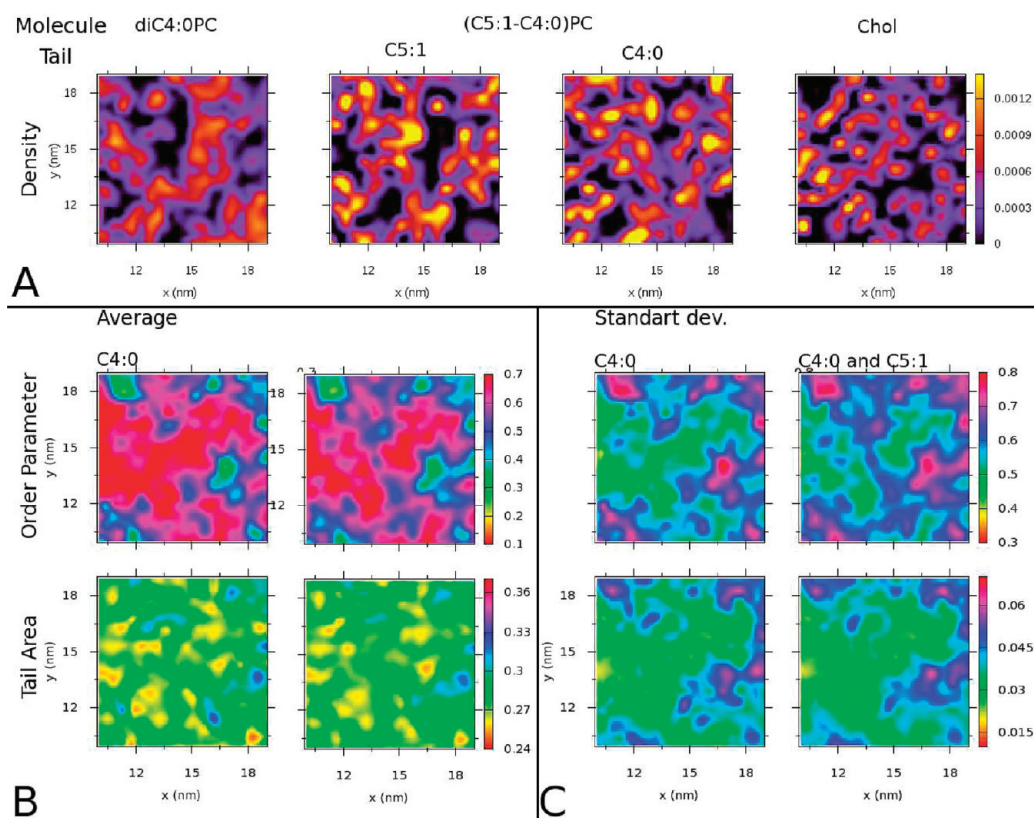

Figure 13. Surface plots for 35:35:30 (C5:1-C4:0)PC:diC4:0PC:Chol mixtures. Details are the same as in Figure 11.

In addition, we observed that the asymmetric chain structure of the unsaturated lipids can influence their orientation. As described, the mixed membranes containing these lipids show one phase with composition fluctuations of increasing

3535

dx.doi.org/10.1021/jp212406u | *J. Phys. Chem. B* 2012, 116, 3525−3537
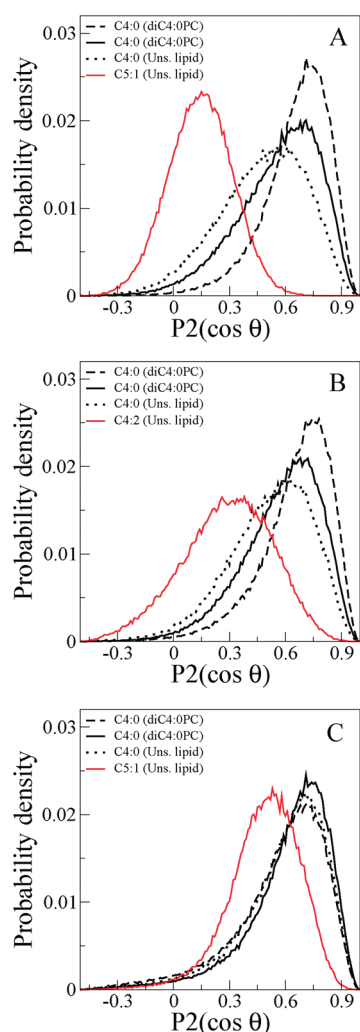
Figure 14. Distribution of the orientational order parameter in ternary mixtures with cholesterol, diC4:0PC, and (C5:4-C4:0)PC (A), (C4:2-C4:0)PC (B), or (C5:1-C4:0)PC (C). Curves represent the unsaturated (red lines) or saturated (black dotted lines) tails that belong to the asymmetric lipid, or the C4:0 tails (black solid lines) of diC4:0PC. The dashed black lines show the distribution for the saturated tails of diC4:0PC in mixtures with 30% cholesterol and 35% of the symmetric unsaturated lipids diC5:4PC (A), diC4:2PC (B), or diC5:1PC(C).

magnitude with the degree of unsaturation. Although the lateral structure of the bilayers is transient and fluctuating, a short length structure develops from the nonrandom orientation of the asymmetric lipids in these short-living clusters. The saturated tails tend to overlap with regions enriched in saturated lipids and cholesterol; meanwhile, the polyunsaturated chains are preferentially oriented against those regions. Two conditions were found to enhance the anisotropic orientation: one is the degree of unsaturation, and the other is a decrease of temperature that reduces the rotational entropy. Moreover, cholesterol follows a nonhomogeneous gradient, which is consistent with its greater affinity for saturated phospholipids acyl chains.[47−49] The gradient of cholesterol, together with the preferred orientation of the asymmetric lipids, increases the number of contacts of cholesterol with the saturated tails over the unsaturated tails of the asymmetric polyunsaturated PC. These results are in line with experimental observations in bilayer mixtures with cholesterol and asymmetric lipids that

inferred a closer interaction of cholesterol with the saturated tails. Those works proposed some short-range arrangement of the molecules to explain the observations.[48,49] Our simulations show that in bilayers with the monounsaturated lipids, the nematic order of the saturated chain of either the asymmetric lipid or the saturated lipid is almost the same. Meanwhile, the saturated chain of the asymmetric polyunsaturated lipids becomes progressively more disordered than the saturated PC chains, as the number of unsaturations increases. Moreover, the greatest configurational order is reached in the liquid-ordered separated domains. The small clusters of polyunsaturated lipids disrupt the tight packing of the liquid ordered phase.

The mismatch between one and the other tail of the asymmetric lipid is enhanced with the degree of unsaturation, and, as mentioned before, we found always only a minor mismatch between the saturated tail of the asymmetric PC and the chains of the fully saturated lipid. On the other hand, the gradient of conformational order increases toward regions enriched in the densely packed cholesterol and saturated PC. Together, these observations indicate that the orientation of the asymmetric lipid would put into contact tails with reduced mismatch and favor the alineation of saturated tails at the edge of unsaturated lipid clusters. It is conceivable that this will improve the acyl chain interactions.

Finally, the orientation adopted by the asymmetric polyunsaturated lipids suggests that they could stabilize the interface of domains. A recent work using the MARTINI CG model found that small proportions (2%) of asymmetric monounsaturated lipids can behave as linactants, decreasing the line tension at the liquid-ordered liquid-disordered domain boundary. Nevertheless, they reported that asymmetric polyunsaturated lipids have a partitioning behavior similar to the symmetric polyunsaturated lipid and show almost no preference for the interface.[27] Interestingly, this behavior could change if they were the major low-melting component, as proposed theoretically,[25] a condition encountered for asymmetric lipids in natural membranes. In this case, the entropy of mixing that drives the lipids to the bulk phase would be overcome.

We found preliminarily that increasing the mismatch between the saturated and unsaturated asymmetric lipids eventually induces the separation of phases, and we are currently working to measure the free energy contribution of the reorientation of the asymmetric lipids at the domain boundaries. A very interesting point to elucidate is if this contribution is of the order magnitude of the line tension.

■ AUTHOR INFORMATION

Corresponding Author
*E-mail: rosetti@tandar.cnea.gov.ar.

Notes
The authors declare no competing financial interest.

■ REFERENCES

(1) Marrink, S. J.; de Vries, A. H.; Mark, A. E. *J. Phys. Chem. B* **2004**, *108*, 750.
(2) Singer, S. J.; Nicolson, G. L. *Science* **1972**, *175*, 720.
(3) Engelman, D. M. *Nature* **2005**, *438*, 578.

(4) Plowman, S. J.; Muncke, C.; Parton, R. G.; Hancock, J. F. *Proc. Natl. Acad. Sci. U.S.A.* **2005**, *102*, 15500.

(5) Sharma, P.; Varma, R.; Sarasij, R. C.; Gousset, I. K.; Krishnamoorthy, G.; Rao, M.; Mayor, S. *Cell* **2004**, *116*, 577.

(6) Veatch, S. L.; Keller, S. L. *Biophys. J.* **2003**, *85*, 3074.

(7) Kusumi, A.; Koyama-Honda, I.; Suzuki, K. *Traffic* **2004**, *5*, 213.

(8) Mayor, S.; Rao, M. *Traffic* **2004**, *5*, 231.

(9) Edidin, M. *Trends Cell. Biol.* **2001**, *11*, 492.

(10) Fan, J.; Sammalkorpi, M.; Haataja, M. *FEBS Lett.* **2010**, *584*, 1678.

(11) Honerkamp-Smith, A. R.; Veatch, S. L.; Keller, S. L. *Biochim. Biophys. Acta* **2009**, *1788*, 53.

(12) Yethiraj, A.; Weisshaar, J. C. *Biophys. J.* **2007**, *93*, 3113.

(13) Zhao, J.; Wu, J.; Heberle, F. A.; Mills, T. T.; Klawitter, P.; Huang, G.; Constanza, G.; Feigenson, G. W. *Biochim. Biophys. Acta* **2007**, *1768*, 2764.

(14) Veatch, S. L.; Keller, S. L. *Phys. Rev. Lett.* **2005**, *94*, 148101.

(15) Pokorny, A.; Yandek, L. E.; Elegbede, I. E.; Hinderliter, A.; Almeida, P. F. F. *Biophys. J.* **2006**, *91*, 2184.

(16) Almeida, R.; Loura, L. M. S.; Fedorov, A.; Prieto, M. *J. Mol. Biol.* **2005**, *346*, 1109.

(17) Shaikh, S. R.; Brzustowicz, M. R.; Gustafson, N.; Stillwell, W.; Wassall, S. R. *Biochemistry* **2002**, *41*, 10593.

(18) Zhao, J.; Wu, J.; Shao, H.; Kon, F.; Jain, N.; Hunt, G.; Feigenson, G. *Biochim. Biophys. Acta* **2007**, *178*, 2777.

(19) Heberle, F. A.; Wu, J.; Lin Goh, S.; Petruzielo, R. S.; Feigenson, G. W. *Biophys. J.* **2010**, *99*, 3309.

(20) Konyakhina, T. M.; Lin Goh, S.; Amazon, J.; Heberle, F. A.; Wu, J.; Feigenson, G. W. *Biophys. J.* **2011**, *101*, L08.

(21) Soni, S. P.; LoCascio, D. S.; Liu, Y.; Williams, J. A.; Bittman, R.; Stillwell, W.; Wassall, S. R. *Biophys. J.* **2008**, *95*, 203.

(22) Filippov, A.; Oradd, G.; Lindblom, G. *Biophys. J.* **2007**, *93*, 3182.

(23) Brewster, R.; Pincus, P. A.; Safran, S. A. *Biophys. J.* **2009**, *97*, 1087.

(24) Brewster, R.; Safran, S. A. *Biophys. J.* **2010**, *98*, L21.

(25) Yamamoto, T.; Brewster, R.; Safran, S. A. *Europhys. Lett.* **2004**, *67*, 321.

(26) Yamamoto, T.; Safran, S. A. *Soft Matter* **2011**, *7*, 7021.

(27) Schäfer, L. V.; Marrink, S. J. *Biophys. J.* **2010**, *99*, L91.

(28) de Joannis, J.; Coppock, P. S.; Yin, F.; Mori, M.; Zamorano, A.; Kindt, J. T. *J. Am. Chem. Soc.* **2010**, *133*, 3625.

(29) Niemela, P. S.; Ollila, S.; Hyvonen, M. T.; Karttunen, M.; Vattulainen, I. *PLoS Comput. Biol.* **2007**, *3*, 304.

(30) Aittoniemi, J.; Niemela, P. S.; Hyvonen, M. T.; Karttunen, M.; Vattulainen, I. *Biophys. J.* **2007**, *92*, 1125.

(31) Pandit, S. A.; Vasudevan, S.; Chiu, S. W.; Mashl, R. J.; Jakobsson, E.; Scott, H. L. *Biophys. J.* **2004**, *87*, 1092.

(32) Martinez-Seara, H.; Róg, T.; Karttunen, M.; Vattulainen, I.; Reigada, R. *PLoS One* **2010**, *5*, e11162.

(33) Pandit, S. A.; Jakobsson, E.; Scott, H. L. *Biophys. J.* **2004**, *87*, 3312.

(34) Marrink, S. J.; Risselada, H. J.; Yefimov, S.; Tieleman, D. P.; de Vries, A. H. *J. Phys. Chem. B* **2007**, *111*, 7812.

(35) Risselada, H. J.; Marrink, S. J. *Proc. Natl. Acad. Sci. U.S.A.* **2008**, *105*, 17367.

(36) Tumaneng, P. W.; Pandit, S. A.; Zhao, G.; Scott, H. L. *J. Chem. Phys.* **2010**, *132*, 065104.

(37) Marrink, S. J.; de Vries, A. H.; Harroun, T. A.; Katsaras, J.; Wassall, S. *J. Am. Chem. Soc.* **2008**, *130*, 130.

(38) van der Spoel, D.; Lindahl, E.; Hess, B.; Groenhof, G.; Mark, A. E.; Berendsen, H. J. C. *J. Comput. Chem.* **2005**, *26*, 1701.

(39) Berendsen, H. J. C.; Postma, J. P. M.; Van Gunsteren, W. F.; Dinola, A.; Haak, J. R. *J. Chem. Phys.* **1984**, *81*, 3684.

(40) Rycroft, C. H.; Grest, G. S.; Landry, J. W.; Bazant, M. Z. *Phys. Rev. E* **2006**, *74*, 021306 ; http://math.lbl.gov/voro++.

(41) Frenkel, D.; Smit, B. *Understanding Molecular Simulation*, 2nd ed.; Academic Press: San Diego, CA, 2002.

(42) Marrink, S. J.; Risselada, J.; Mark, A. E. *Chem. Phys. Lipids* **2005**, *135*, 223.

(43) Marsh, D. *Biochim. Biophys. Acta* **2009**, *1788*, 2114.

(44) Domański, J.; Marrink, S. J.; Schäfer, L. V. *Biochim. Biophys. Acta* **2011**, *1818*, 984.

(45) Harroun, T. A.; Katsaras, J.; Wassall, S. R. *Biochemistry* **2006**, *45*, 1227.

(46) Bennett, W. F. D.; MacCallum, J. L.; Hinner, M. J.; Marrink, S. J.; Tieleman, D. P. *J. Am. Chem. Soc.* **2009**, *131*, 12714.

(47) Pitman, M. C.; Suits, F.; MacKerell, A. D.; Feller, S. E. *Biochemistry* **2004**, *43*, 15318.

(48) Huster, D.; Arnold, K.; Gawrisch, K. *Biochemistry* **1998**, *37*, 17299.

(49) Brzustowicz, M. R.; Cherezov, V.; Caffrey, M.; Stillwell, W.; Wassall, S. R. *Biophys. J.* **2002**, *82*, 285.

(50) Feller, S. E.; Gawrisch, K.; MacKerell, A. D. Jr. *J. Am. Chem. Soc.* **2001**, *124*, 318.

(51) Saiz, L.; Klein, M. L. *Biophys. J.* **2001**, *81*, 204.

(52) Huber, T.; Rajamoorthi, K.; Kurze, V. F.; Beyer, K.; Brown, M. F. *J. Am. Chem. Soc.* **2001**, *124*, 298.

(53) Rosetti, C. M.; Pastorino, C. *J. Phys. Chem. B* **2010**, *115*, 1002.

(54) Stillwell, W.; Wassall, S. R. *Chem. Phys. Lipids* **2003**, *126*, 1.

(55) Perlmutter, J. D.; Sachs, J. N. *J. Am. Chem. Soc.* **2011**, *133*, 6563.

(56) Schick, M., arXiv:1111.2350v1 [cond-mat.soft] (2011).